Local structural changes in excited $Ti^{3+}:Al_2O_3$ studied by time-resolved XANES

E. Vorobeva,[1] S. L. Johnson,[1] P. Beaud,[1] C. J. Milne,[2] M. Benfatto,[3] and G. Ingold[1]
[1]*Swiss Light Source, Paul Scherrer Institute, CH-5232 Villigen, Switzerland*
[2]*Laboratoire de Spectroscopie Ultrarapide, Ecole Polytechnique Fédérale de Lausanne, CH-1015 Lausanne, Switzerland*
[3]*Laboratori Nazionali di Frascati dell'INFN, CP 13, 00044 Frascati, Italy*
(Received 4 March 2009; revised manuscript received 21 August 2009; published 6 October 2009)

Transient changes in the local structure of optically excited Ti^{3+} ions in a Al_2O_3 single crystal are studied by time-resolved x-ray absorption spectroscopy. A model considering coupling of the excited $^2E(C_{3v})$ electronic state of the Ti^{3+} ion to the approximate $A_{1g}(O_h)$ and $E_g(O_h)$ local vibrational modes of the TiO_6 octahedron is constructed to fit the experimental data. We determine the magnitude of the $A_{1g}(O_h)$ mode and give an estimate of the $E_g(O_h)$ Jahn-Teller distortion although this analysis does not distinguish between compression and elongation of the oxygen octahedron. Assuming a compressed octahedron, the $E_g(O_h)$ distortion is found to be 0.14 ± 0.02 Å with an $A_{1g}(O_h)$ mode of 0.066 ± 0.006 Å. In the case of an elongated octahedron the $E_g(O_h)$ distortion is -0.195 ± 0.017 Å with an $A_{1g}(O_h)$ mode of 0.052 ± 0.002 Å.

DOI: 10.1103/PhysRevB.80.134301 PACS number(s): 61.05.cj, 78.47.−p, 63.20.kd, 71.70.Ej

Electronic excitation of impurity ions in crystals is often accompanied by transient changes in the local structure of the host. These changes are most commonly studied by optical spectroscopy, yielding indirect and sometimes incomplete information. Quantitative information about the short- and medium-range organization of atoms can be provided by x-ray absorption spectroscopy (XAS). The element specificity of this method is ideal for the study of substitutional impurity centers in solids. In the case of very dilute impurities, collecting extended x-ray absorption fine-structure (EXAFS) spectra with a good signal-to-noise ratio can be a challenging task. In such cases, the larger features of x-ray absorption near-edge structure (XANES) are often exploited to yield information about the local structure. Analysis of XANES spectra is, however, not straightforward because of the photoelectron multiple-scattering processes that contribute significantly to the near-edge region. Pump-probe methods can be used to study the transient XAS created in the course of chemical reactions or due to electronic excitation of solids.[1] This technique has been successfully applied to investigate the electronic and geometric modifications of photoexcited chemicals in solution although progress in this field is limited due to the limited short x-ray pulse flux available at current sources.[2–6]

To evaluate the quality of information that we obtain from the analysis of transient XAS data of dilute laser-excited impurities in crystalline solids, we have chosen $Ti^{3+}:Al_2O_3$ as a model system. $Ti^{3+}:Al_2O_3$ has been studied extensively from analysis of optical, magnetic, Raman, and neutron data as an example of a crystal with a strong Jahn-Teller (JT) electron-lattice coupling in the excited $^2E(C_{3v})$ state. The electronic level structure of the Ti^{3+} ion in Al_2O_3 is sketched in Fig. 1. The cubic crystal-field splits the $3d^1$ ^2D term into a doublet $^2E_g(O_h)$ and a triplet $^2T_{2g}(O_h)$. The ground $^2T_{2g}(O_h)$ term is split further by the trigonal crystal field into a singlet $^2A_1(C_{3v})$ and doublet $^2E'(C_{3v})$. Here, the prime indicates that the doublet $^2E'$ originates from a three-dimensional representation $^2T_{2g}$ of the O_h point group. Strong electron-phonon coupling in the excited $^2E(C_{3v})$ state causes a tetragonal distortion of the oxygen octahedron, stabilizing the complex in one of the three configurations (the static Jahn-Teller effect).[7,8] As a result, the doublet $^2E(C_{3v})$ splits into $^2E_{1/2}(C^*_{3v})$ and $^2E_{3/2}(C^*_{3v})$ sublevels, where $^2E_{1/2}$ and $^2E_{3/2}$ label irreducible representations of the C^*_{3v} double group. The Jahn-Teller interaction in the ground $^2E'(C_{3v})$ state is weak and at room temperature the complex easily undergoes transitions among these three configurations on the time scale of the experiment (the dynamic Jahn-Teller effect). As a result the XAS of unexcited $Ti^{3+}:Al_2O_3$ shows no evidence of this tetragonal distortion.

To quantify the distortion of the local structure when the Ti^{3+} ion is in the excited $^2E_{3/2}(C^*_{3v})$ state, we performed time-resolved laser pump/x-ray probe measurements. The setup and the experimental geometry are shown in Fig. 2. The sample, a single sapphire crystal with 0.45 wt. % of Ti^{3+} ions was cut so that the angle between the surface and the optical C_3 axis was 29.5°. To excite the sample, the output of a regenerative femtosecond laser amplifier (800 nm, 110 fs, 1 kHz) was converted with an optical parametric amplifier to a wavelength of 500 nm, near the peak of the Ti^{3+} absorption band. To avoid damage to the sample we decreased the peak intensity of the pump pulse by stretching the pulses to approximately 350 fs by transmission through a 15 cm quartz rod. We then focused the π-polarized beam incident at Brewster's angle (29.5° from the surface) to a 80×60 μm spot on the crystal surface, simultaneously minimizing reflection losses and maximizing absorption of the Ti^{3+} by aligning the electric field polarization of the refracted beam with the crystal C_3 axis.[9] The pulse energy was 160 μJ, corresponding to a laser fluence of 3.33 J/cm^2. The XAS of the excited Ti^{3+} ions was probed in the vicinity of the Ti K edge by a focused synchrotron x-ray beam (50×5 μm). The π-polarized x-rays entered the crystal at an angle of approximately 20° from the surface, making the polarization of the x-rays 40° from the crystal C_3 axis. A silicon avalanche photodiode collected x-ray fluorescence from the Ti^{3+} ions. A boxcar integrator measured the intensity of the fluorescence signal over a 100 ns time window at a controlled delay with respect to the pump pulse. Further experimental details are described in Ref. 10. This setup has been used previously to measure

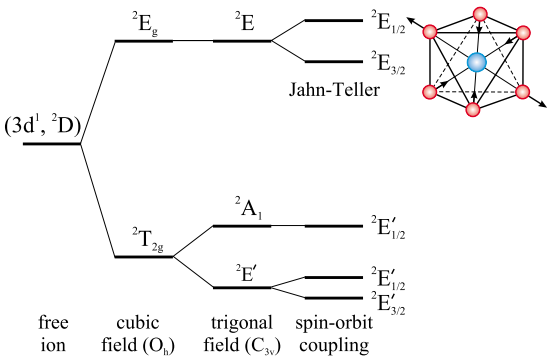

FIG. 1. (Color online) Electronic structure of the Ti^{3+} ions in the Al_2O_3 crystal.

transient x-ray absorption spectra from laser-excited chemicals in solutions.[5,10]

The initial excitation of the Ti^{3+} ion by the laser to the $^2E(C_{3v})$ state is followed by fast nonradiative relaxation to the $^2E_{3/2}(C^*_{3v})$ sublevel which occurs within 3.5 ps.[11] The population of the $^2E_{3/2}(C^*_{3v})$ state at room temperature lives for several microseconds. At 50 ns after the laser pulse, when all the species are in the lower sublevel of the $^2E(C_{3v})$ doublet, we have observed transient changes in the titanium *K*-edge XANES spectrum associated with the alteration of the bond lengths of the ligands caused by the strong Jahn-Teller interaction (inset on Fig. 3). The magnitude of the changes in the spectrum is approximately 2% of the titanium *K*-edge jump. We performed the measurements at 50 ns and 1 μs after the laser excitation but we found no significant difference between the spectra.

We also measured the time dependence of the transient XAS at 4981 and 5000 eV at room temperature. The results, together with the time dependence of optical fluorescence from the sample originating from the $^2E_{3/2}(C^*_{3v})$ level, are shown in Fig. 3. The exponential relaxation of the photoinduced change occurs with a time constant of 1.8 ± 0.1 μs, distinctly shorter than the room-temperature optical-fluorescence lifetime of 3.2 μs. This difference is likely explained by thermal quenching caused by heating of the near-surface region of the crystal from laser excitation. The

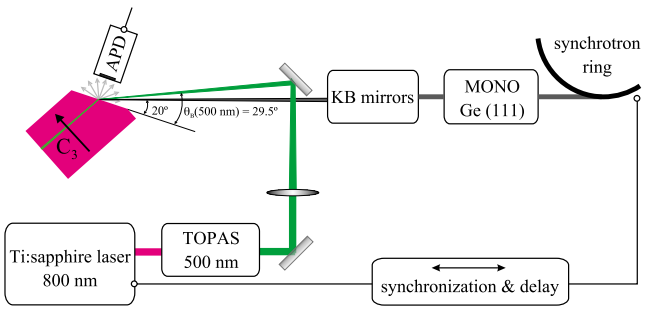

FIG. 2. (Color online) Experimental setup and geometry of the laser pump—x-ray probe experiment. The π-polarized laser beam is incident at Brewster's angle 29.5° from the surface and the π-polarized monochromatic x-rays enter the crystal at an angle of approximately 20° from the surface. The x-ray fluorescence signal is collected with a silicon avalanche photodiode.

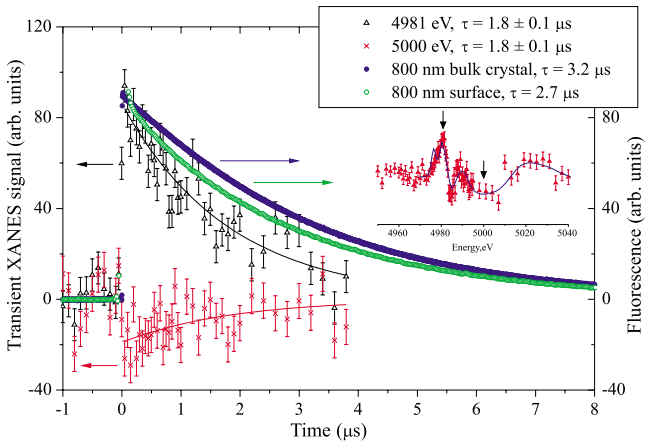

FIG. 3. (Color online) Time decay of Ti^{3+}:Al_2O_3 fluorescence originating from the excited $^2E_{3/2}(C^*_{3v})$ level at 300 K from the bulk crystal τ=3.2 μs (●) and from the near-surface region τ=2.7 μs (○); time dependence of the transient XAS effect at 50 ns after the laser pulse at 4.981 keV (△) and 5 keV (×), τ=(1.8+/−0.1) μs. The inset shows the transient XANES spectrum and the arrows indicate where the kinetics data were taken.

lifetime of 1.8 μs would correspond to a crystal temperature of 375 K.[9] To test this hypothesis, we measured the optical-fluorescence lifetime when the signal is collected from the near-surface region only. A 1 mm diameter pin hole was attached to a polished surface of the crystal. A π-polarized laser beam incident at a Brewster's angle (60.5°) was focused on the surface in the center of the pin hole and the fluorescence signal was collected with a photodiode at approximately 45° from the crystal surface, collecting light emitted at depths up to approximately 370 μm. Under these experimental conditions we measured the fluorescence signal with a decay constant of 2.7 μs, whereas the luminescence signal from the bulk sample decays with a time constant of 3.2 μs. The approximately 30% higher laser fluence in the x-ray experiment and the much shallower probe depth of the x-ray beam (approximately 15 μm) may explain the further shortening of the decay constant to 1.8 ± 0.1 μs.

I. GROUND-STATE STRUCTURE

Corundum has a trigonal Bravais lattice with a space group of $R\bar{3}c$. The trigonal unit cell contains two Al_2O_3 units. The local structure of the aluminum atoms is an octahedron of oxygen atoms distorted along a trigonal axis with a C_3 local symmetry, commonly approximated in the literature by a C_{3v} point group.[12] The octahedron is characterized by two different Al-O interatomic distances. The rhombohedral lattice constant is a_R=5.128 Å and α=55.333°; the aluminum atoms are in 4*c* symmetry sites with x=0.352 and the oxygen atoms are in 6*e* symmetry sites with x=0.556.[13]

Incorporation of a Ti^{3+} impurity ion causes a distortion of the local structure since the ionic radius of Ti^{3+} in the octahedral site (r^{3+}_{Ti}=0.670 Å) is greater than the aluminum ionic radius (r^{3+}_{Al}=0.535 Å).[14] This structural relaxation around the Ti^{3+} impurity in α-Al_2O_3 was determined by Gaudry *et al.*[15] by combining XANES experiments and *ab initio* calcula-

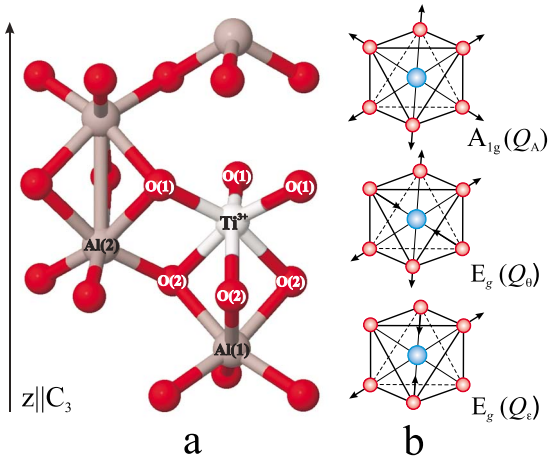

FIG. 4. (Color online) (a) The unit cell of the $Ti^{3+}:Al_2O_3$ and (b) the $A_{1g}(O_h)$ and $E_g(O_h)$ normal modes of the octahedral complex.

tions. According to their results, the impurity site symmetry is preserved; the Ti^{3+} site is still described by the C_3 point group, characterized by two different Ti-O distances. The distances within the first coordination shell of the impurity are increased by 0.13 Å for Ti-O(1) and by 0.08 Å for Ti-O(2). The Ti^{3+} ion itself is displaced away from the Al(1) atom by 0.03 Å [Fig. 4(a)].

II. ELECTRONIC STRUCTURE AND THE JAHN-TELLER EFFECT

In $Ti^{3+}:Al_2O_3$ the atoms in the first coordination shell of the titanium impurity form a nearly octahedral environment with a trigonal distortion along the C_3 axis. This trigonal distortion is, however, less than 5% of the average Ti-O bond lengths and we will therefore simplify the following discussion by using the eigenvectors of the undistorted octahedral complex (O_h point group) to describe the local vibrational modes. For the same reason we also neglect coupling of the excited $^2E(C_{3v})$ to the trigonal vibrational modes and do not include them in the analysis of the excited-state structure. Any distortion of an octahedral complex is determined by atomic displacements along the x, y, and z axes for each of the six atoms. In the first approximation only even displacements can change the potential energy of a complex. In the cubic representation the A_{1g}-symmetry vibrational mode can be described as $\Delta Q_A = Q_A \cdot (\mathbf{r}_1+\mathbf{r}_2+\mathbf{r}_3+\mathbf{r}_4+\mathbf{r}_5+\mathbf{r}_6)/\sqrt{6}$. The $E_g(O_h)$ mode has two normal components assigned as θ and ε: $\Delta Q_\theta = Q_\theta \cdot (2\mathbf{r}_1+2\mathbf{r}_4-\mathbf{r}_2-\mathbf{r}_5-\mathbf{r}_3-\mathbf{r}_6)/\sqrt{12}$ and $\Delta Q_\varepsilon = Q_\varepsilon \cdot (\mathbf{r}_2+\mathbf{r}_5-\mathbf{r}_3-\mathbf{r}_6)/2$; where Q_A, Q_θ, and Q_ε are the magnitudes of the $A_{1g}(O_h)$ and $E_g(O_h)$-symmetry distortions, respectively, $\mathbf{r}_i$ is a unitary displacement along the Ti-O_i bond vector. These normal modes are shown schematically in Fig. 4(b).

The electronic states of the d^1-like ions in octahedral complexes are known to interact with tetragonal lattice vibrations. In $Ti^{3+}:Al_2O_3$ crystal the distortion of the oxygen octahedron along one of the tetragonal axes when the Ti^{3+} is in the $^2E(C_{3v})$ excited state is responsible for the emission-absorption Stokes shift[16] and for the quenching of the fluorescence at high temperatures.[17,18] A detailed analysis of radiative and nonradiative transitions in $Ti^{3+}:Al_2O_3$ is given by Grinberg *et al.*,[19,20] assuming that the local structure of the Ti^{3+} is a perfect octahedron. A two-dimensional configuration-coordinate space model was constructed to fit experimental spectroscopic and time-resolved luminescence data. The authors assumed that the dominant lattice distortion is the $E_g(O_h)$ mode and that the distortion occurs only along the configuration coordinate Q_θ.

When the Ti^{3+} ion is in the ground $^2E'(C_{3v})$ state, the oxygen octahedron is distorted along one of the three quasi-fourfold axes,[19] although due to the relatively weak electron-phonon coupling the distortion is small. As the JT energy of the ground state ($\sim$130 cm^{-1}) and the energy of thermal vibrations at room temperature ($\sim$200 cm^{-1}) are comparable, the system is not localized in either of the three equivalent minima. Coupling of the ground $^2E'(C_{3v})$ electronic state of the Ti^{3+} ion to the local trigonal vibrational modes can be neglected as it is quenched by the spin-orbit interaction.[21]

When the Ti^{3+} ion is excited to the $^2E(C_{3v})$ state the octahedron is stressed along one of the fourfold axes and the $^2E(C_{3v})$ doublet is split into $^2E_{1/2}(C^*_{3v})$ and $^2E_{3/2}(C^*_{3v})$ sublevels (Fig. 1). In this case the coupling to the local $E_g(O_h)$ mode is much stronger (the estimated JT energy is 2900 cm^{-1}) and the system is frozen in one of three possible configurations. As there is no global preference for a particular orientation, our experimental data contain a superposition of all three normal tetragonal spectra. The minimum of the potential corresponding to the excited $^2E_{3/2}(C^*_{3v})$ state is shifted in the configuration-coordinate space over the minimum of the ground $^2E'(C_{3v})$ state potential. The position of the minimum of the excited-state potential, corresponding to the best and most reliable reproduction of the optical data, is found to be at $Q_\theta \approx 5.5\sqrt{\hbar/M\omega}$ where M is a reduced mass of the ions involved and $\hbar\omega$ is a phonon energy.[19] Assuming a simple cluster model consisting of one central titanium ion and six oxygen ions located in the vertices of a perfect octahedron, $M = 26.56 \times 10^{-27}$ kg (a mass of a single oxygen atom). Taking the average phonon frequency in the excited state of 200 cm^{-1} (Ref. 19) as an effective frequency of the local $E_g(O_h)$ mode, we get an estimate for the displacement in the configuration-coordinate space $Q_\theta \approx 0.561$ Å, which is a very large fraction of the bond distance. The local cluster model used to obtain this estimate does not explicitly consider potentially significant effects arising from the coupling of these local vibrational modes of the impurity to the phonon spectrum of the crystal.

III. FIT TO THE GROUND-STATE XANES SPECTRUM

A quantitative analysis of the experimental data was performed using the MXAN fitting procedure, designed to fit x-ray absorption data from the edge up to about 200 eV above the absorption edge and to recover information about the symmetry and atomic distances of the nearest neighbors of the absorber.[22–26]

As a starting point for calculations we used the corundum structure[12] with a distorted first shell as given in Ref. 15. To determine the optimal cluster size, we performed a series of single-trial calculations increasing the number of scatterers at each step with fixed structural parameters. It was found that including more than 80 scattering atoms does not introduce significant changes in the spectrum. This corresponds to a cluster size of 5.57 Å, consisting of 45 oxygen, 35 aluminum, and one titanium atom as an absorber. A cluster of the same size was used previously to calculate the structural relaxation around Ti^{3+} impurity.[15] For such a large supercell interaction between impurities belonging to neighboring clusters can be neglected.

In our calculations we used the Hedin-Lunqvist real potential convolved with a phenomenological energy-dependent Lorentzian broadening function.[24] For optimization of the ground-state structure we allowed only atomic motions which preserve the trigonal local point symmetry of the Ti^{3+} ion. The static XANES spectrum and the best fit to the data are shown in Fig. 5(a). All the features in the spectrum are well reproduced in the fit except for the one around 5007 eV although it is present in the best-fit spectrum before convolution with the broadening function [dashed curve in Fig. 5(a)]. Within the uncertainties the optimized atomic positions in the first shell are found to be the same as those calculated by Gaudry *et al.*[15] with the PARATEC code.

IV. FIT TO THE TRANSIENT XANES SPECTRUM

To account for the transient heating of the probed region of the sample to 375 K, we first expanded the optimized crystal structure obtained from the fit to the static XANES spectrum by 0.1%, using an accepted value of 19×10^{-6} K^{-1} for the linear expansion coefficient of corundum.[27] We then applied a radial distortion of the first coordination shell corresponding to the Q_θ coordinate of the $E_g(O_h)$ symmetry vibrational mode [Fig. 4(b)]. We calculated with the MXAN code three normal spectra (corresponding to Q_θ distortion along the three equivalent directions), averaged these together, and then subtracted the original static spectrum to obtain a model for the transient XAS. We found that $E_g(O_h)$ mode alone was not sufficient to reproduce even the correct sign of the transient spectrum [Figs. 5(b) and 5(c)]. As a next step we incorporated a fully symmetrical expansion/compression of the local octahedron, equivalent to an $A_{1g}(O_h)$ mode. This mode was not considered in the analysis of the optical and electron-spin resonance spectroscopic data because it produces no vibronic splittings and has almost no impact on the spectra.[21] We ran a least-square minimization procedure based on the Levenberg-Marquardt algorithm. For the fit we optimized three parameters: the magnitude of the $E_g(O_h)$ mode Q_θ, the magnitude of the $A_{1g}(O_h)$ mode, Q_A and the excitation yield. The excitation yield of the sample is relevant to the analysis of our data, as it serves as a scaling factor for the transient spectrum. Figure 6 shows the reduced χ^2 optimized for the excitation yield with fixed values of the Q_θ and Q_A. Negative values of the Q_θ correspond to elongation of the octahedron. One can see that there are two roughly equivalent local minima around $Q_\theta \approx \pm 0.17$ Å and $Q_A \approx 0.07$ Å. The parameters for the best fit obtained with these values of the initial parameters and the reduced χ^2 values of the fit are listed in Table I; the experimental transient spectrum and the fit spectra are shown in Figs. 5(b) and 5(c). Although the quality of the fit is better for elongated geometry, it is not possible to distinguish reliably between elongation and compression of the oxygen octahedron from this analysis.

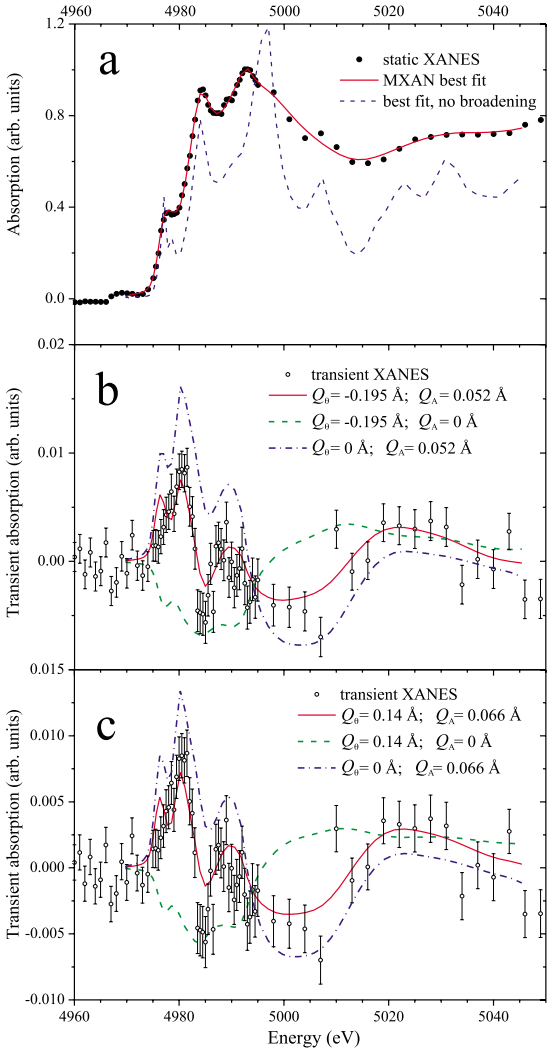

FIG. 5. (Color online) (a) Static XANES spectrum of $Ti^{3+}:Al_2O_3$ at 300 K (●); the MXAN fit to the data (—) and the MXAN fit spectrum before convolution with a phenomenological energy-dependent Lorentzian broadening function (- - -). (b) The difference between the excited and unexcited spectra at 50 ns after the laser pulse (○); fit to the transient data for elongated geometry of the oxygen octahedron: $Q_\theta = -0.195 \pm 0.017$, $Q_A = 0.052 \pm 0.002$ Å, excitation yield $= 11 \pm 1\%$ (—); the transient spectrum calculated for $A_{1g}(O_h)$ distortion only (-·-·-) and the transient spectrum calculated for $E_g(O_h)$ distortion only (- - -); (c) the difference between the excited and unexcited spectra at 50 ns after the laser pulse (○); fit to the transient data for compressed geometry of the oxygen octahedron: $Q_\theta = 0.14 \pm 0.02$ Å, $Q_A = 0.066 \pm 0.006$ Å, excitation yield $= 8.1 \pm 0.8\%$ (—); the transient spectrum calculated for $A_{1g}(O_h)$ distortion only (-·-·-) and the transient spectrum calculated for $E_g(O_h)$ distortion only (- - -).

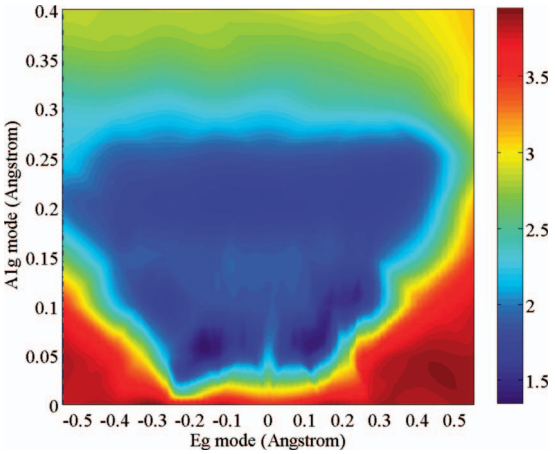

FIG. 6. (Color) The χ^2_ν of the fit to the transient XANES spectrum of $Ti^{3+}:Al_2O_3$ optimized for the excitation yield versus magnitudes of the $A_{1g}(O_h)$ and $E_g(O_h)$ local vibrational modes. Negative values of the $E_g(O_h)$ mode correspond to the elongation of the octahedron.

The Jahn-Teller distortion in the excited $^2E(C_{3v})$ state is found to be 0.14 ± 0.02 Å (for compression) or -0.195 ± 0.017 Å (for elongation), which is approximately 30% of the value of 0.561 Å estimated from the optical data using a simple cluster model.[18] There are at least two possible reasons for such a discrepancy. First, the model which was used to describe the optical data did not consider coupling of the excited $^2E(C_{3v})$ state to the vibrational $A_{1g}(O_h)$ mode. Although the $A_{1g}(O_h)$ mode produces no extra vibronic splittings, it will contribute to the Stokes shift together with the $E_g(O_h)$ mode. Introduction of the $A_{1g}(O_h)$ mode into the model would result in a smaller magnitude of the $E_g(O_h)$ mode required to fit the configuration-coordinate diagram to the experimental Frank-Condon transitions. Second, the estimate for the energy of the local $E_g(O_h)$ phonon in the excited $^2E(C_{3v})$ state of 200 cm^{-1} is quite small. Values around 400 cm^{-1}, where the peaks in the density of states of the *E*-mode phonons in corundum crystal occur,[28,29] may be more appropriate. For these higher values of the phonon energy, the displacement of the potential minimum in the *E* space will be approximately 30% smaller.

V. CONCLUSION

In this work we have demonstrated a measurement and analysis of the transient changes in the structurally relevant XANES from an optically excited dilute crystal impurity. An account of the $A_{1g}(O_h)$ distortion with respect to the ground state is necessary to achieve a satisfactory fit to the experimental data. From our analysis we estimate the contribution of the $A_{1g}(O_h)$ mode, which is not possible by analyzing only optical- and magnetic-resonance spectroscopic data. We also determine the magnitude of the Jahn-Teller tetragonal distortion in the excited $^2E(C_{3v})$ state of the Ti^{3+} impurity although we are not able to distinguish between elongation and compression of the oxygen octahedron. For compressed geometry the $E_g(O_h)$ mode is found to be 0.14 ± 0.02 Å with the $A_{1g}(O_h)$ mode of 0.066 ± 0.006 Å and in the case of elongation the $E_g(O_h)$ mode is -0.195 ± 0.017 Å with the $A_{1g}(O_h)$ mode of 0.052 ± 0.002 Å.

TABLE I. Parameters obtained from the MXAN fit to the transient XANES spectrum of $Ti^{3+}:Al_2O_3$ for elongated and compressed geometry of the oxygen octahedron.

	Compressed octahedron	Elongated octahedron
$Q_\theta[E_g(O_h)]$, Å	0.14 ± 0.02	-0.195 ± 0.017
$Q_A[A_{1g}(O_h)]$, Å	0.066 ± 0.006	0.052 ± 0.002
Excitation yield	0.081 ± 0.008	0.11 ± 0.01
χ^2_ν	1.48	1.44

The results show that it is indeed possible to extract structural information from transient XANES of these types of systems, containing information otherwise hidden from optical spectroscopy. Significant improvements to the quality of this information must likely require measurements over a much wider energy range with a signal-to-noise ratio sufficient for transient EXAFS analysis.

ACKNOWLEDGMENTS

The experiments were performed on the μXAS beamline at the Swiss Light Source, Paul Scherrer Institut, Villigen, Switzerland. We are grateful to Andreas Hauser and Philip Tregenna-Piggott for fruitful discussion and μXAS beamline scientists Daniel Grolimund and Camelia Borca whose efforts have made these experiments possible. We also acknowledge the usage of x-ray facilities at the Laboratory for Developments and Methods, Paul Scherrer Institut, Villigen, Switzerland.

[1] C. Bressler and M. Chergui, Chem. Rev. **104**, 1781 (2004).
[2] L. X. Chen, W. J. H. Jäger, G. Jennings, D. J. Gosztola, A. Munkholm, and J. P. Hessler, Science **292**, 262 (2001).
[3] M. Saes, C. Bressler, R. Abela, D. Grolimund, S. L. Johnson, P. A. Heimann, and M. Chergui, Phys. Rev. Lett. **90**, 047403 (2003).
[4] M. Benfatto, S. Della Longa, K. Hatada, K. Hayakawa, W. Gawelda, C. Bressler, and M. Chergui, J. Phys. Chem. B **110**, 14035 (2006).
[5] W. Gawelda, Van-Thai Pham, Maurizio Benfatto, Yuri Zaushitsyn, Maik Kaiser, Daniel Grolimund, Steven L. Johnson, Rafael Abela, Andreas Hauser, Christian Bressler, and Majed Chergui1, Phys. Rev. Lett. **98**, 057401 (2007).
[6] C. Bressler, C. Milne, V.-T. Pham, A. ElNahhas, R. M. van der Veen, W. Gawelda, S. Johnson, P. Beaud, D. Grolimund, M. Kaiser, C. N. Borca, G. Ingold, R. Abela, and M. Chergui, Sci-

ence **323**, 489 (2009).
[7] J. H. Van Vleck, J. Chem. Phys. **7**, 72 (1939).
[8] U. Opik and M. H. L. Pryce, Proc. R. Soc. Lond. A Math. Phys. Sci. **238**, 425 (1957).
[9] P. F. Moulton, J. Opt. Soc. Am. B **3**, 125 (1986).
[10] M. Saes, F. van Mourik, W. Gawelda, M. Kaiser, M. Chergui, and C. Bressler, Rev. Sci. Instrum. **75**, 24 (2004).
[11] S. K. Gayen, W. B. Wang, V. Pertricevic, K. M. Yoo, and R. R. Alfano, Appl. Phys. Lett. **50**, 1494 (1987).
[12] C. A. Bates and J. P. Bentley, J. Phys. C **2**, 1947 (1969).
[13] R. W. G. Wyckoff, *Crystal Structures: Inorganic Compounds RXn, RnMX2, RnMX3* (John Wiley & Sons, New York, 1964), Vol. 2:.
[14] R. D. Shannon, Acta Crystallogr. A **32**, 751 (1976).
[15] E. Gaudry, D. Cabaret, P. Sainctavit, C. Brouder, F. Mauri, J. Goulon, and A. Rogalev, J. Phys.: Condens. Matter **17**, 5467 (2005).
[16] B. F. Gächter and J. A. Koningstein, J. Chem. Phys. **60**, 2003 (1974).
[17] P. Albers, E. Stark, and G. Huber, J. Opt. Soc. Am. B **3**, 134 (1986).
[18] C. E. Byvik and A. M. Buoncristiani, IEEE J. Quantum Electron. **21**, 1619 (1985).
[19] M. Grinberg, A. Mandelis, K. Fjeldsted, and A. Othonos, Phys. Rev. B **48**, 5922 (1993).
[20] M. Grinberg, A. Mandelis, and K. Fjeldsted, Phys. Rev. B **48**, 5935 (1993).
[21] R. M. Macfarlane, J. Y. Wong, and M. D. Sturge, Phys. Rev. **166**, 250 (1968).
[22] M. Benfatto and S. Della Longa, J. Synchrotron Radiat. **8**, 1087 (2001).
[23] S. Della Longa, A. Arcovito, M. Girasole, J. L. Hazemann, and M. Benfatto, Phys. Rev. Lett. **87**, 155501 (2001).
[24] M. Benfatto, S. Della Longa, and C. R. Natoli, J. Synchrotron Radiat. **10**, 51 (2003).
[25] M. Benfatto, A. Congiu-Castellano, A. Daniele, and S. Della Longa, J. Synchrotron Radiat. **8**, 267 (2001).
[26] M. Benfatto, P. D'Angelo, S. Della Longa, and N. V. Pavel, Phys. Rev. B **65**, 174205 (2002).
[27] T. Goto, O. L. Anderson, I. Ohno, and S. Yamamoto, J. Geophys. Res. **94**, 7588 (1989).
[28] F. Gervais and B. Piriou, J. Phys. C **7**, 2374 (1974).
[29] H. Bialas and H. J. Stolz, Z. Phys. B **21**, 319 (1975).